Article

Not peer-reviewed version

Petrographic and Geo-Mechanical Characteristics of Inzari Formation of Nizampur Basin, Nowshera District, Khyber Pakhtunkhwa, Pakistan

Hassan Ayaz , Jaincong Xu * , Muhammad Usama Aslam , Sohail Ahmad , Junaid Ali

Posted Date: 16 September 2024

doi: 10.20944/preprints202409.1216.v1

Keywords: inzari formation; geo-mechanical characteristics; petrography characteristic; building material; Nizampur basin

Article

Petrographic and Geo-Mechanical Characteristics of Inzari Formation of Nizampur Basin, Nowshera District, Khyber Pakhtunkhwa, Pakistan

Hassan Ayaz [1], Jaincong Xu [1,*], Muhammad Usama Aslam [1], Sohail Ahmad [1] and Junaid Ali [2]

[1] College of Civil Engineering, Tongji University, Shanghai 200092, China;
[2] College of Meteorology, Comsats University, Islamabad, Pakistan; 2393163@tongji.edu.cn (H.A.); xjc1008@tongji.edu.cn (J.X.); usamaasalam98@tongji.edu.cn (U.A.); sohail_ahmad@tongji.edu.cn (S.A.); ja3904081@gmail.com (J.A.)
* Correspondence: xjc1008@tongji.edu.cn

Abstract: This study is focus on the petrographic properties and geo-mechanical properties of the Inzari formation rocks at Tar Khel Village, District Swabi, Khyber Pakhtunkhwa, and whether they are suitable for use as building materials for structures like bridges, buildings, and roads. Five fresh and large samples have been taken from various areas of this formation. These rock samples were identified as siliciclastic mudstone through a careful petrographic analysis. The test result of physical properties (water absorption, specific gravity, and porosity) and mechanical properties (unconfined compression strength, unconfined tensile strength, Schmidt hammer test, and shear strength) of these rock samples shows as follows: their unconfined compressive strength with between 23 to 94 MPa, their specific gravity values being very high (≥2.78), and their porosity and water absorption values being very low (<1%), imply that the Inzari formation rock can be used as an excellent building material. The rock sample strength variations may be mainly caused by the presence and abundance of stylolite and fractures. Furthermore, the petrographic property analysis of these rock samples indicates that they have the significant amount of micrite and calcite, which are suitable to be use as both asphalt and concrete aggregate. According to this study, the Inzari formation rock is appropriate for use as fine aggregate in concrete, asphalt, and other building materials.

Keywords: inzari formation; geo-mechanical characteristics; petrography characteristic; building material; Nizampur basin

1. Introduction

Rock aggregates have been used in numerous construction industries. Geological studies on rocks can help to enhance the quality, life expectancy, and security of civil structures such as bridges, highways, passageways, and dam. The strength of rock is primarily determined by its mechanical and physical characteristics. The geo-mechanical actions of rocks as building materials have been extensively investigated [1,2]. The geo-mechanical characteristics of rock are often the action consequence of multiple related factors, including petrology, mineralogy, texture and form, erosion, permeability, and fractures [3]. When rocks are used in the building construction, they must follow several physical and mechanical criteria in the building industry. The main factors that determine the physical characteristics of rock are its texture, petrological characteristics, geological structures, and surrounding conditions. Additional, petrographic characteristics affect the geotechnical reactions of building materials [4] To comprehend their behavior, it is necessary to consider how rocks react to various petrographic features, which include grain size, shape, orientation, and fractures.

When classifying rocks, the aforementioned petrographic traits are rarely taken into consideration. The current study also investigates how they affect the strength of rocks [5]. The term "index properties or parameters that govern the composition of rock to support its classification" refers to the physical characteristics of rock. The mechanical features referred to as strength are the parameters or attributes that tell us about a rock's strength and durability under specific

 doi:10.20944/preprints202409.1216.v

circumstances like humidity, temperature, and loading conditions. In addition to the rock's inherent physical and chemical characteristics, non-technical methods of rock excavation used in the construction industry additionally have an impact on the strength of rock. The properties of building materials differ based on the kind of rock, and are significantly impacted by the processes involved in the creation of rock in addition to the outside influences that exist all through the rock's metamorphism [6].

A geologist is needed to assess the characteristics and quality of rock during extraction and determine whether it will be feasible to use it for a particular construction project. As a result, evaluating an aggregate's quality is crucial to deciding whether or not it can be utilized for engineering purposes[7]. It is required to subject rock aggregates to a variety of tests in accordance with international and local regulations in order to determine their suitability for any engineering-related purpose. These tests include the uniaxial compressive stress test (UCS), tensile strength, Brazilian test, Schmidt's hammer test, point load index (PLI), SD test, total core recovery (TCR), and rock quality designation (RQD), in addition to porosity, water absorption, specific gravity, and density. The nature of rock often is examined using microscopic analysis (polarizing and scanning electron microscopes) and physical and chemical studies. In addition to being utilized as building materials, rock aggregates are employed in the construction of railways, roads, and dams, as well as for concrete aggregate and asphalt base courses.

As a result, a lot of academics have attempted to investigate how certain petrographically and rock fabric characteristics affect the mechanical qualities of rocks [8]. Rock fabric and petrographic factors such as grain size, form, degree of cementation, type of cementation between grains, and mineralogical composition all affect mechanical properties. Soil and rocks are the two categories of earth materials that engineering geology studies [9]. Soil and rocks can be utilized as building materials in surface excavations such as railroad cuts, roadways, dams, and canals. Both can be utilized as sources of raw materials for construction products (aggregates, decorative stones, building stones, etc.). Margala limestone has been utilized as aggregate by Pakistan's National Highway Authority (NHA) for the building of motorways and highways in major projects. Margala limestone has been used as an aggregate resource for the making of roads as well as a general building material.

In this study, the primary goal is to determine whether Inzari formation rocks in the Nizampur basin are suitable for construction thorough the petrography and physical-mechanical studies of the acquired rock samples. This study will also aid new economic and major infrastructural growth throughout the area, particularly as they connect to the China-Pakistan Economic Corridor (CPEC).

2. Geological Setting

The study area (shown in Figure 1) is situated at Tar Khel village in District Nowshera, Pakistan, where is also a typical Inzari formation (see Figure 2). It is located at latitude 33º 50'31.69" N and longitude 72º 09'10.48" E. It is situated about 97 km from Peshawar and about 135 km from Islamabad. Geologically, the three different tectonic plates exist in northern Pakistan (Figure 3), ellipse shows the location of study area (Figure 3), which includes the Eurasian plate, the Kohistan Island arc (KIA), and the Indian plate. During the early Cretaceous period (130 million years ago), the Kohistan Islands arc (KIA/KLIA), an intra-oceanic arc inside the Tethys Ocean, first collided with the Eurasia plate via the Main Karakoram Thrust (MKT), also known as the Shyok Sutures or Northren Suture Zone [10]. The Indus suture zone, also known as the Main Mantle Thrust, was created by the beginning to the mid-Eocene collision of the KIA with the Indian plate (MMT). This collision resulted in the KIA being hidden or abducted onto the Indian plate rocks. Despite being an intra-oceanic island, the KIA is joined to the Asian/Eurasian plate along its northern suture and the Indo-Pakistan plate along its southern suture. The evolution of KLIA/KIA is well acknowledged and understood.

The exact moment of the KLIA's collision with the Asian plate and Indo-Pakistan remains debatable nonetheless. Pakistan has several large thrust faults extending from north to south. The thrust system that divides the Kohistan Island Arc (KIA) complex in the south from the deformed meta-sedimentary and igneous rocks of the Asian Land mass in the north is headed by the Main Karakoram thrust. The Kohistan Islands Arch is constrained through the Main Mantle Thrust [11].

 doi:10.20944/preprints202409.1216.v

The Hazara -Kashmir Syntaxis is a prominent bend produced by the Main Boundary Thrust that extends east-west along the vast majority of the foreland basin before turning northward west of the Jhelum River. The Hazara and Murree Faults, which border the northern edges of the Kala- Chitta and Hazara Categories, are thought to be associated with the Main Boundary Thrust.

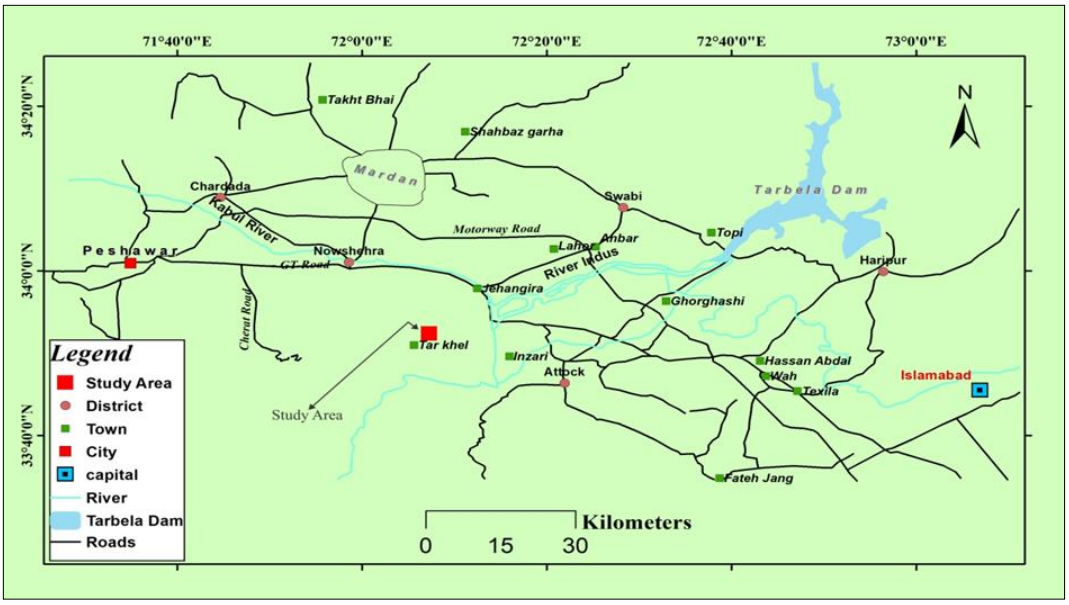

Figure 1. Location of the study area.

The Hissartang Fault divides the Indian Plate into two distinct zones. The term "internal metamorphosed zone" refers to the northern region between the Hissartang Fault and MMT, whereas the term "external unmetamorphosed zone" or "low-grade metamorphic zone" describes the southern region. These strata are separated from Tertiary foreland basin deposits further to the south by the Main Boundary Thrust (MBT). The Himalayas are split into Tethys Himalayas, Higher Himalayas, Lesser Himalayas, and Outer Himalayas according to with north to south orientation. Between the Kala Chitta Range to the south and the Peshawar Basin to the east is the Attock-Cherat Range (ACR). The Hissartang Thrust in the Nizampur basin, which separates the southern slab of the ACR from the Kala Chitta Range, marks the border between the ACR and the range. The ACR and Kala Chitta Range rocks cracked because of movement along the Hissartang thrust. Sediments from the Paleocene Pre-Cambrian are outcropping in the ACR.

 doi:10.20944/preprints202409.1216.v

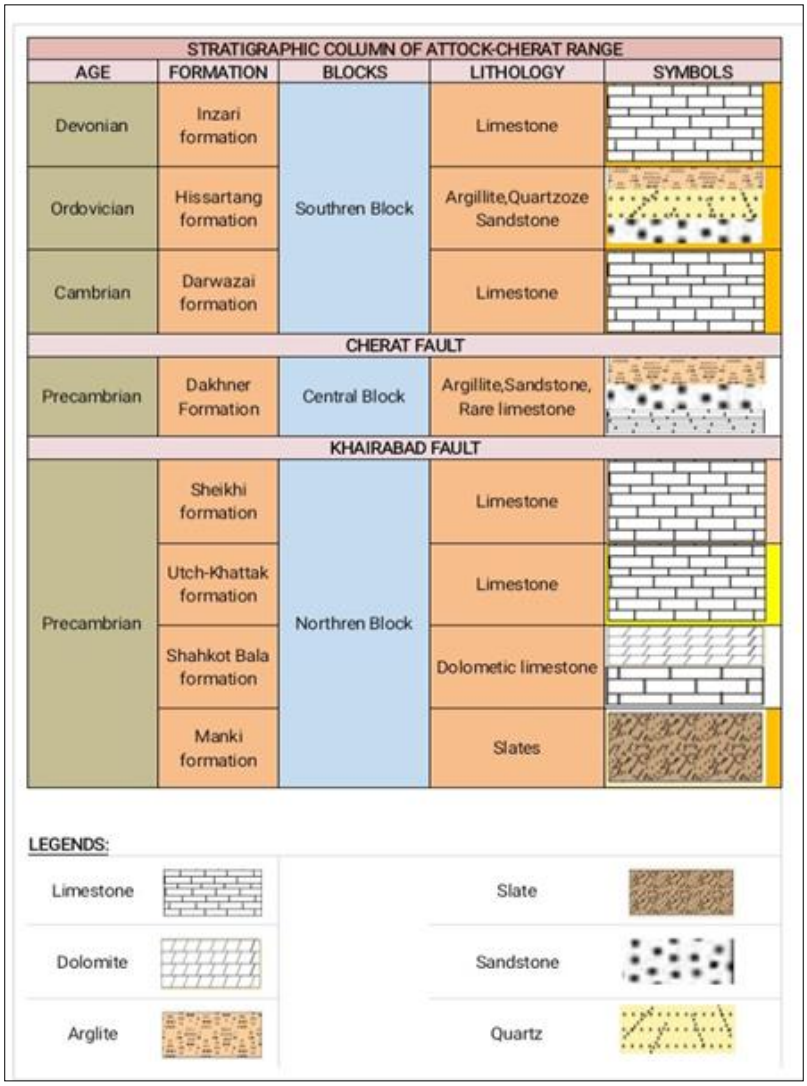

Figure 2. Stratigraphic column from the Attock-Cherat Range.

 doi:10.20944/preprints202409.1216.v

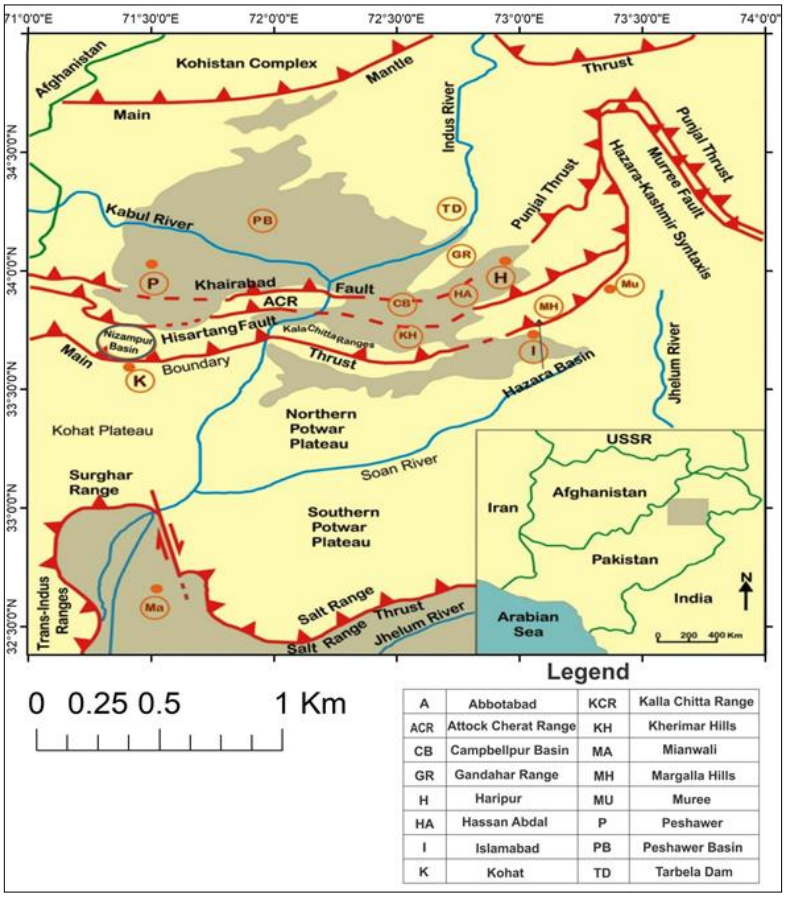

Figure 3. Generalized tectonic map of Northern Pakistan [12].

The Kahi Gorge is located in Khyber Pakhtunkhwa, in northwest Pakistan, on the foothills of the Himalayas in the Nizampur Valley. The Kala Chitta Range (KCR) is a segment of the active Himalayan Foreland Fold-and-Thrust Belt, which has been gradually thrust southward along the Main Boundary Thrust (MBT) in a sequence of top-to-south thrust imbricates, creating the Northern Pakistani region's fault system [13].

3. Methodology

The methodology and techniques used in this study are shown in Figure 4

 doi:10.20944/preprints202409.1216.v

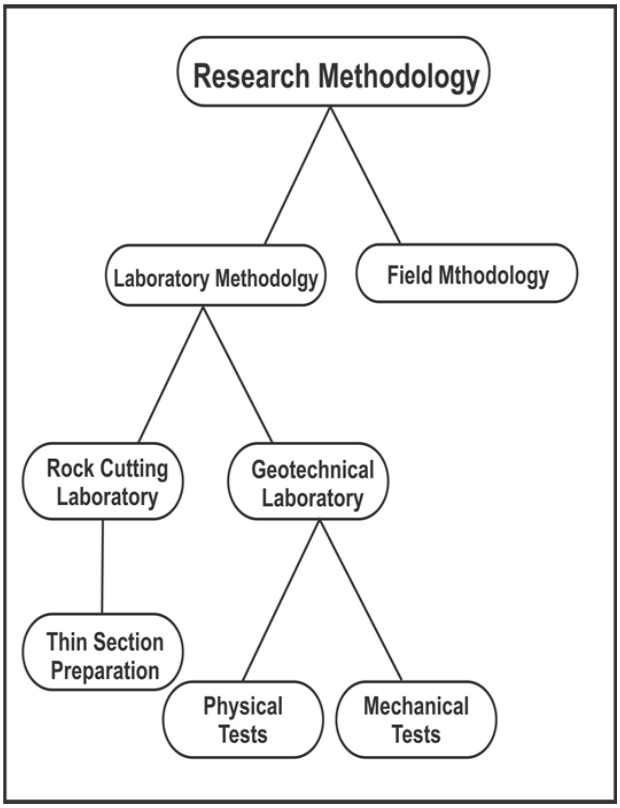

Figure 4. Flow charts representing the methodology.

3.1. Field Methodology

The typical Inzari formation, which is situated in Nizampur Village in District Nowshera, Pakistan, was the site of a geological field study (see Figure 5). These rocks are located close to Cherat and Nowshera, at the base of the Khattak Mountains Range. To the northeast lie the villages of Hisartang. Five fresh 20–30-kilogram bulk samples were gathered from various locations. The bulk samples were gathered to ascertain the petrographic and physico-mechanical characteristics of the Inzari formation rocks. These samples had the numbers marked on them. Every sample's location was recorded via GPS. Approximately one kilogram of random specimens was taken for a detailed physical-mechanical and petrographic investigation of the exposed lithology of the Inzari formation [14]. To conduct more analysis, the materials were moved to the rock cutting.

 doi:10.20944/preprints202409.1216.v

Figure 5. The typical Inzari formation in Nizampur Village, District Nowshera, Pakistan.

3.2. Laboratory Methodology

Five bulk rock specimens collected in the field were sent to the lab to be analyzed geotechnically and petrographically. The ASTM requirements were followed in the preparation of the sample cores (see Figure 6). Uniaxial compressive strength, unconfined tensile strength (UTS), shear strength, absorption of water, Schmidt hammer, specific gravity, and water absorption were among the engineering characteristics of the selected samples that were assessed [15].

3.3. Geotechnical Laboratory

Rock strength was determined by conducting experiments of undamaged and undisturbed materials [16]. According to the process shown in (Figure 7), the physical and mechanical tests of rocks were carried out on specimens in the laboratory, shown in (Figure. 7).

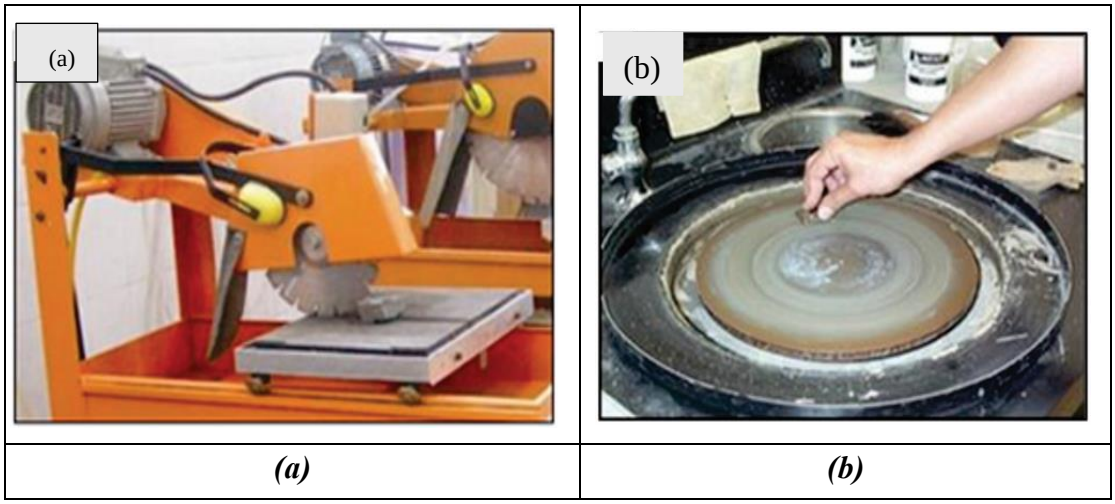

Figure 6. Preparation of the sample cores **(a)** Cutting of the rock sample into chip size through rock cutting machine; **(b)** Polishing of the chip sized sample with grinding machine.

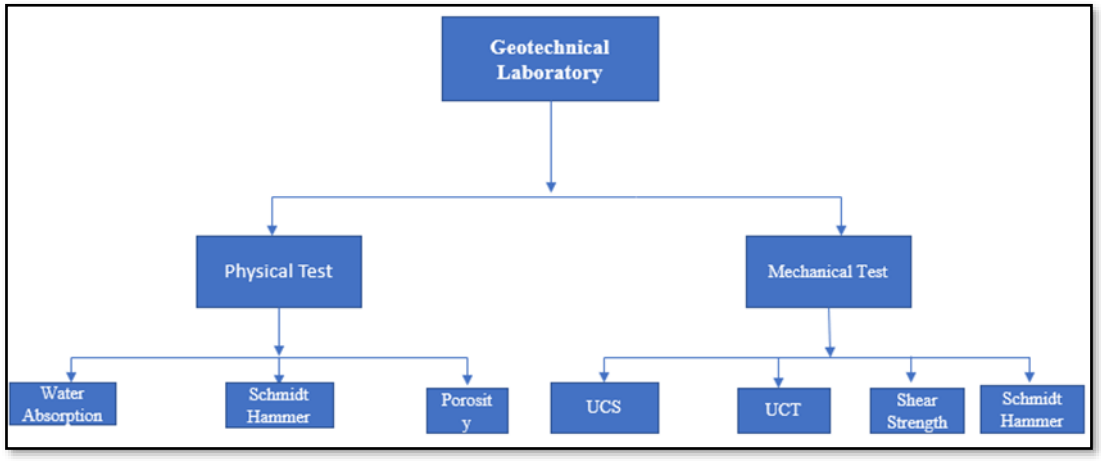

Figure 7. Flow charts of rock physical and mechanical tests.

 doi:10.20944/preprints202409.1216.v

4. Results and Discussions

4.1. Physico - Mechanical Properties

4.1.1. Unconfined Compressive Strength or Uniaxial Strength

The maximum stress that a specimen will endure is known as the unconfined compressive strength (UCS) denoted by Formula (1), which is unidirectional stress that is applied to a rock sample. When determining whether rock is suitable to be the construction material, its toughness a measure of its ability to withstand weathering and maintain its original size, shape, strength, and appearance for an extended length of time, should be considered. It is commonly accepted that rocks with a compressive strength of 35 MPa are appropriate for building stones. The compression strength of the tested rock samples was measured by using the direct approach with a strength testing machine in this study. The width and length of the cube sample are both 3 inches, shown in (Figure 8). The UCS test were conducted for three specimens from each bulk sample. Figure 8 shows how the cube samples were inserted into the strength testing apparatus and how the force was applied continuously without creating a shock wave. Table 1 and (Figure 9) provide the UCS test result of the tested samples. Formula (1) was used to calculate the compressive strength without confinement.

Formula (1) was used to calculate the compressive strength without confinement.

$$UCS = P/A \qquad (1)$$

Where,

P = Load of rock failure (kN)

A = Rock sample cube's cross-sectional area (m^2)

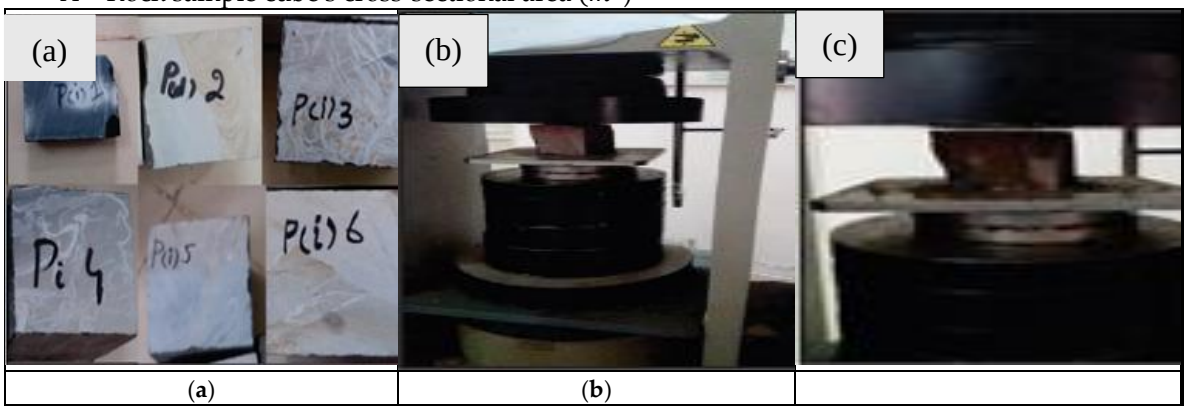

(**a**) (**b**)

Figure 8. Rock unconfined compressive strength test (a) Representative cube samples used for unconfined compressive strength test; (b) Cube sample loaded in strength testing machine for measuring UCS; (c) Fracturing of a core sample during UCS testing.

Table 1. Unconfined compressive strength test result of the studied samples.

Sample number	Cube sample	Diameter		Area		Load		Strength	
		in	m	in^2	m^2	Ibf	ton	psi	MPa
Pi1	Pi1(a)	2.25"	0.05	4.0	0.002	13235	6.61	3309	23
Pi2	Pi2(a)	3.28″	0.08	8.5	0.005	43590	21.79	5128	35
	Pi2(b)	3.28″	0.08	8.5	0.005	44212	22.10	5201	36
	Pi2(c)	3.28″	0.08	8.5	0.005	87930	43.96	10345	71
Pi3	Pi3(a)	3.28″	0.08	8.5	0.005	78179	39.08	9198	63
	Pi3(b)	3.28″	0.08	8.5	0.005	92526	46.26	10885	75
	Pi3(c)	3.28″	0.08	8.5	0.005	85567	42.78	10067	69
	Pi4(a)	3.28″	0.08	8.5	0.005	63284	31.64	7445	51

 doi:10.20944/preprints202409.1216.v

Pi4	Pi4(b)	3.28″	0.08	8.5	0.005	95640	47.82	11252	78
	Pi4(c)	3.28″	0.08	8.5	0.005	115501	57.75	13588	94
Pi5	Pi5(a)	2.22″	0.05	4.0	0.002	13435	6.71	3359	23
	Pi5(b)	2.22″	0.05	4.0	0.002	14224	7.11	3556	25
	Pi5(c)	3.28″	0.08	8.5	0.005	84322	42.16	9920	68
Pi6	Pi6(a)	3.28″	0.08	8.5	0.005	92490	46.24	10881	75
	Pi6(b)	3.28″	0.08	8.5	0.005	59687	29.84	7022	48
	Pi6(c)	3.28″	0.08	8.5	0.005	85114	42.55	10013	69

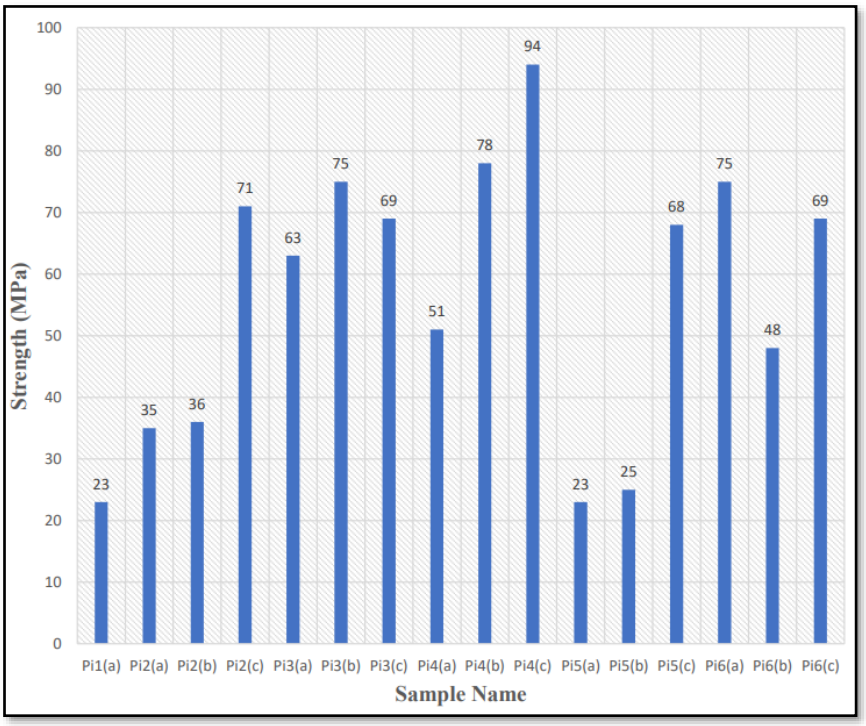

Figure 9. Unconfined compressive strength of the studied samples.

4.1.2. Porosity

One of the important physical attributes that controls the strength and deformation of rocks is their porosity, which is the volume of all the voids and pores in a rock. The size, shape, and mineralogical makeup of the grains—most notably the amount of clay minerals—all have an impact on the porosity of rocks [17]. Rock strength gradually decreases as the degree of porosity rises. It is likely that porosity will change inversely with specific gravity and directly with water absorption. The porosity of the studied samples has a value between 0.27 and 1.32 (see Figure 10 and Table 2). Rock strength decreases as the percentage of porosity increases. Using a saturation approach, the porosity of the specimens was calculated using Formula (2).

$$\text{Porosity} = \left(\frac{w_1 - w_3}{w_1 - w_2}\right) \times 100 \qquad (2)$$

Where,

w_1 = weight in the air
w_2 = weight in water
w_3 = oven dry weight

 doi:10.20944/preprints202409.1216.v

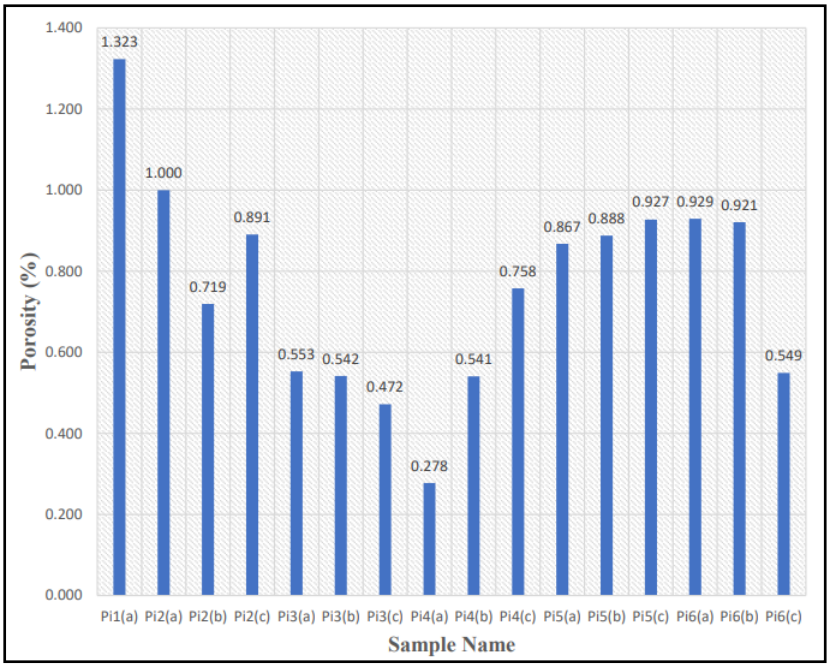

Figure 10. Porosity of the studied samples.

Table 2. Porosity of the studied samples.

Sample number	Cube sample	Weight in air (W_1)	Weight in water (W_2)	Oven dry weight (W_3)	Porosity
Pi 1	Pi 1(a)	370.26	232.27	368.75	1.323
Pi 2	Pi2(a)	905.80	569.24	903.95	1.000
	Pi2(b)	961.49	604.15	960.21	0.719
	Pi2(c)	931.97	585.99	929.89	0.891
Pi 3	Pi3(a)	942.35	592.35	941.24	0.553
	Pi3(b)	959.33	603.47	957.89	0.542
	Pi3(c)	963.07	605.55	961.88	0.472
Pi 4	Pi4(a)	961.24	605.09	960.67	0.278
	Pi4(b)	961.92	604.79	959.72	0.541
	Pi4(c)	944.91	593.34	943.13	0.758
Pi 5	Pi5(a)	395.1	247.94	394.24	0.867
	Pi5(b)	940.53	590.23	938.52	0.888
	Pi5(c)	923.13	580.71	921.59	0.927
Pi 6	Pi6(a)	939.93	585.34	938.19	0.929
	Pi6(b)	910.19	567.51	909.56	0.921
	Pi6(c)	923.15	593.15	922.78	0.549

4.1.3. Water Absorption

 doi:10.20944/preprints202409.1216.v

One of the most important physical features in determining the aggregate's quality is its ability to absorb water. The amount of water a rock absorbing in one day is commonly called water absorption [18]. It is used to adjust the weight of aggregates as a result of water collected in pore spaces. When it exceeds the acceptable limit, the material's characteristics may alter. The investigated samples' average absorption of waterfalls between 0.03 and 0.22, shown in (Figure 11) and Table 3. The weight of rock specimen in the water and its oven-dry weight measured in the laboratory, were the two fundamental prerequisites for figuring out how much water it absorbs. The specimens' absorption capacity was calculated using Formula (3).

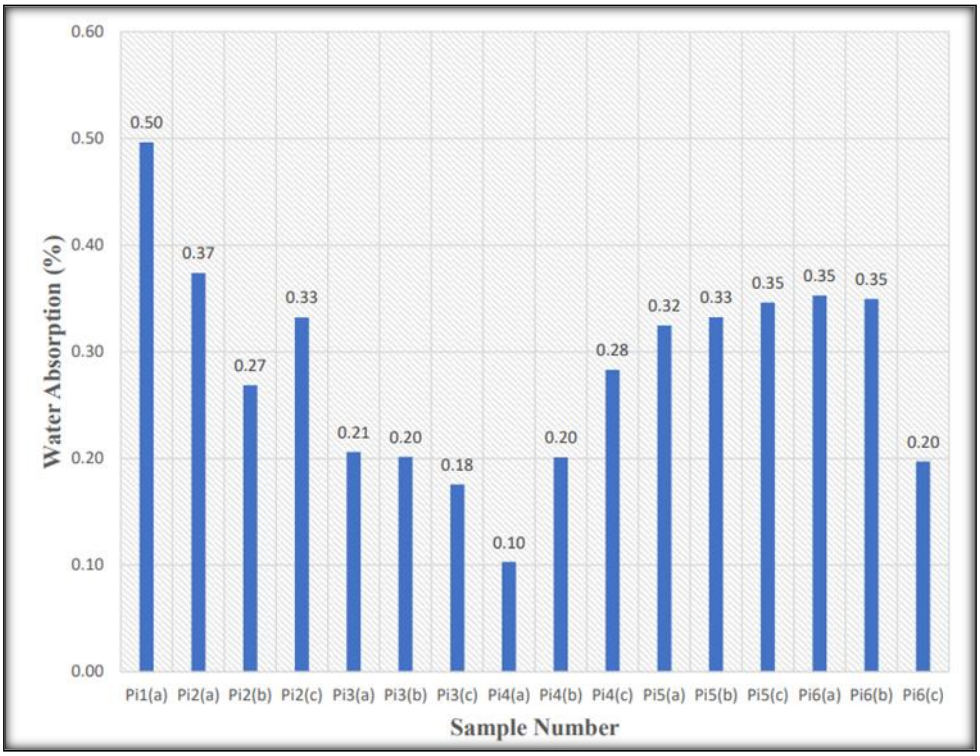

Figure 11. Water absorption values for the studied sample.

$$Percentage\ Absorption = \frac{Absorption}{w_3 \times 100} \quad (3)$$

Where,

$Absorption = w_1 - w_3$

w_1= weight in the air

w_3= oven dry weight

4.1.4. Specific Gravity

The ratio of the density of a material (mass per unit of volume) to that of water is known as specific gravity. Relative density in relation to water is known as specific gravity. After conducting a number of compressive softening tests on engineering materials, it was discovered that the source of rock samples affected the amount of softening they experienced when submerged in water. But they swell gradually, which finally results in a loss of strength and density[19]. Generally, the specific gravity of rocks suitable for large buildings as building materials should be greater than 2.55. Table 4 and (Figure 12) exhibit the samples' specific gravity.

Table 3. Water absorption values for the studied sample.

Sample number	Cube sample	Weight in water (W_1)	Oven dry weight (W_3)	Water absorption	Water absorption (%)

 doi:10.20944/preprints202409.1216.v

Pi1	Pi1(a)	232.27	368.75	1.83	0.50
Pi2	Pi2(a)	569.24	903.95	3.38	0.37
	Pi2(b)	604.15	960.21	2.58	0.27
	Pi2(c)	585.99	929.89	3.09	0.33
Pi3	Pi3(a)	592.35	941.24	1.94	0.21
	Pi3(b)	603.47	957.89	1.93	0.20
	Pi3(c)	605.55	961.88	1.69	0.18
Pi4	Pi4(a)	605.09	960.67	0.99	0.10
	Pi4(b)	604.79	959.72	1.93	0.20
	Pi4(c)	593.34	943.13	2.67	0.28
Pi5	Pi5(a)	247.94	394.24	1.28	0.32
	Pi5(b)	590.23	938.52	3.12	0.33
	Pi5(c)	580.71	921.59	3.19	0.35
Pi6	Pi6(a)	585.34	938.19	3.31	0.35
	Pi6(b)	567.51	909.56	3.18	0.35
	Pi6(c)	593.15	922.78	1.82	0.20

From Table 4 and (Figure 12), it is noted that the specific gravity values of the samples fall between 2.81 and 2.86, indicating that they are better suited for intensive building tasks. The weight of rock specimen in water and the weight of rock specimen in the oven are the two key measurements needed to calculate the specific gravity of rock samples. Each weight of the sample was calculated using Formula (4).

$$Specific\ gravity = \frac{w_3 - w_2}{w_3} \times 100 \qquad (4)$$

Table 4. Specific gravity values for the studied samples.

Sample number	Cube sample	Weight in water (W_2)	Oven dry weight (W_3)	Specific gravity
Pi1	Pi1(a)	232.27	368.75	2.666
Pi2	Pi2(a)	569.24	903.95	2.674
	Pi2(b)	604.15	960.21	2.677
	Pi2(c)	585.99	929.89	2.680
Pi3	Pi3(a)	592.35	941.24	2.683
	Pi3(b)	603.47	957.89	2.688
	Pi3(c)	605.55	961.88	2.687
Pi4	Pi4(a)	605.09	960.67	2.694
	Pi4(b)	604.79	959.72	2.689
	Pi4(c)	593.34	943.13	2.676
Pi5	Pi5(a)	247.94	394.24	2.671
	Pi5(b)	590.23	938.52	2.671
	Pi5(c)	580.71	921.59	2.678
Pi6	Pi6(a)	585.34	938.19	2.634
	Pi6(b)	567.51	909.56	2.635
	Pi6(c)	593.15	922.78	2.784

 doi:10.20944/preprints202409.1216.v

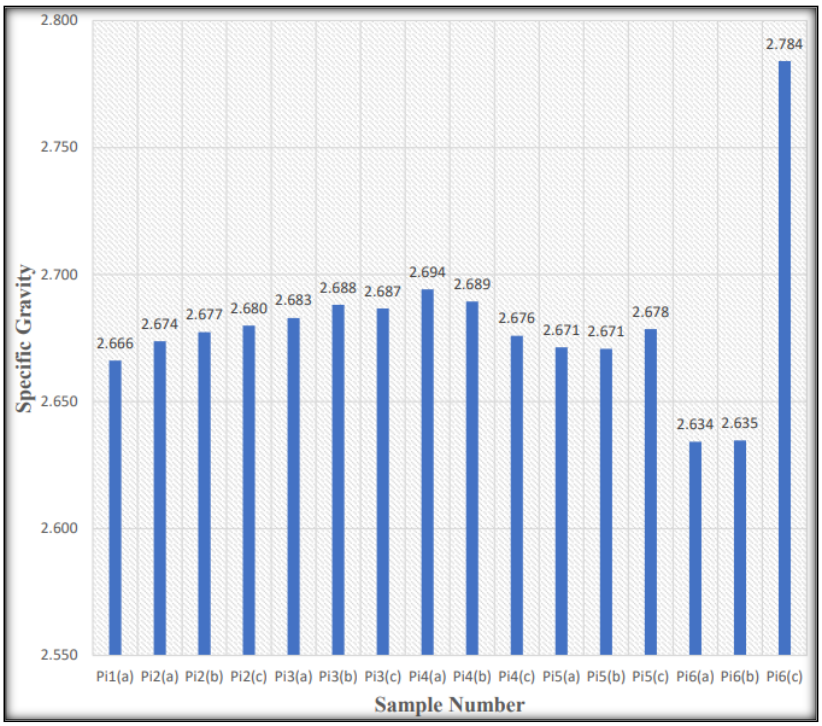

Figure 12. Specific gravity of the studied sample.

4.1.5. Schmidt Hammer Test

The Schmidt hammer test is an established technique to determine the mechanical characteristics of rock material because it offers a rapid, inexpensive, and accurate way to quantify the material hardness. The "Schmidt Hammer Rebound Index" test was designed for testing concrete. It was also used to measure the strength of rock. This inexpensive, non-destructive test additionally offers information about the compressive properties of rock material [20]. The test value is recorded after the Schmidt hammer is released by springing against the rock surface. The range of the average value is 26.5 to 51.0 MPa, shown in Table 5 and (Figure 13).

Table 5. Schmidt hammer test result for the studied rock samples.

Sample number	Cube sample	Schmidt Hammer values
Pi1	Pi1(a)	26.5
Pi2	Pi2(a)	44.7
	Pi2(b)	44.0
	Pi2(c)	46.3
Pi3	Pi3(a)	45.7
	Pi3(b)	46.7
	Pi3(c)	44.7
Pi4	Pi4(a)	41.0
	Pi4(b)	49.7
	Pi4(c)	48.7
Pi5	Pi5(a)	30.0
	Pi5(b)	32.3
	Pi5(c)	51.0
	Pi6(a)	46.3

 doi:10.20944/preprints202409.1216.v

Pi6	Pi6(b)	40.0
	Pi6(c)	43.0

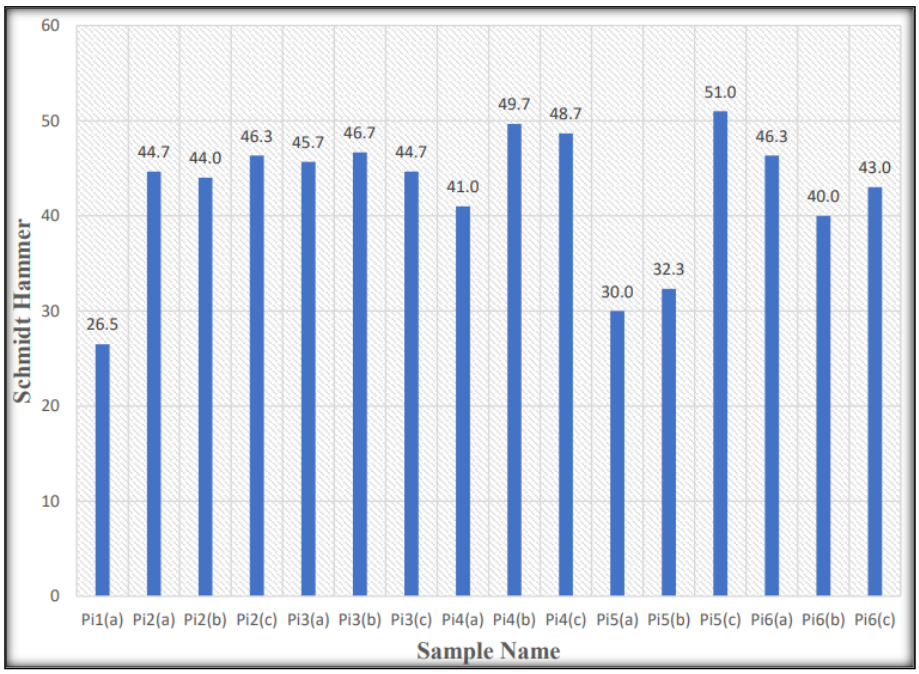

Figure 13. Schmidt Hammer test results of the studied sample.

4.1.6. Shear Strength

The maximum resistance that rock can provide against the deformation when it is continuously sheared owing to shearing action is known as its shear. Torsion testing in a laboratory setting is usually used to evaluate the shear strength of rock specimens. Torsion tests are now a commonly used technique to determine the shear strength of rock samples in labs. For a particular rock, the unconfined tensile strength (UTS) reading was recorded along the negative x-axis, and the uniaxial compressive stress (UCS) reading was recorded along the positive x-axis according to the scale. Based on the UCS and UTS data, the separate Mohr circles were created, and then a shared tangent was drawn between the resulting circles. The two primary factors used for calculating shear strength are cohesiveness (C) and the angle of internal friction (φ).

4.1.7. Unconfined Tensile Strength (UTS)

The UTS test is conducted by applying a vertical force to create tension along the diameter of a rock disc that is being compressed (Figure 14). UTS can be used to evaluate the tensile strength. It is noteworthy that rocks have greater compression strength than tensile strength. The inability to grasp the specimen securely without generating bending forces has frequently made it impossible to quantify tensile strength directly. The ultimate tensile strength (UTS) is calculated by Formula (5).

 doi:10.20944/preprints202409.1216.v

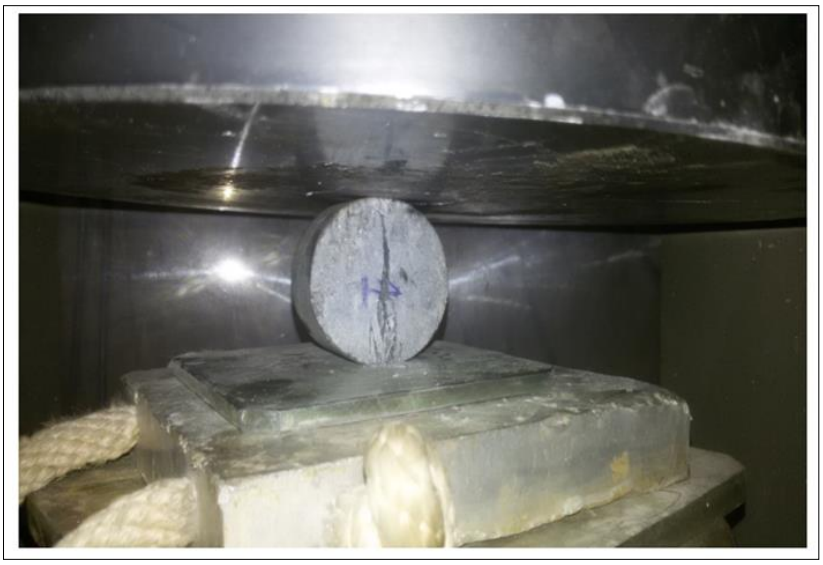

Figure 14. Core sample loading for the unconfined tensile strength (UTS).

$$UST = \frac{2P}{\pi DT} \quad (5)$$

Where,

P = Load (kN)

D =the rock core's diameter

T = the rock core's diameter (m).

4.2. Relationship between the Inzari Formation's Mechanical and Physical Characteristics

To investigate any potential relationships between the various samples of the Inzari formation, their mechanical and physical characteristics are displayed against one another. A significant reduction in the strength of rocks occurs when their void capacity increases. A notable mechanical effect can result from a slight change in the volume of pores [21]. From (Figures 15–17), and Table 6, we are noted that it is typical and predicted for there to be a decrease in porosity and the quantity of water absorbed as the compressive strength rises, and an increase in Schmidt hammer as the compressive strength rises.

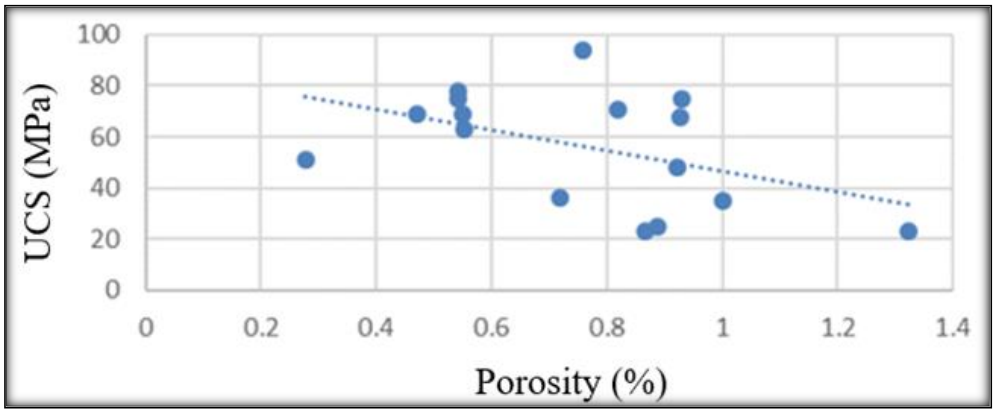

Figure 15. Relation between UCS and porosity.

 doi:10.20944/preprints202409.1216.v

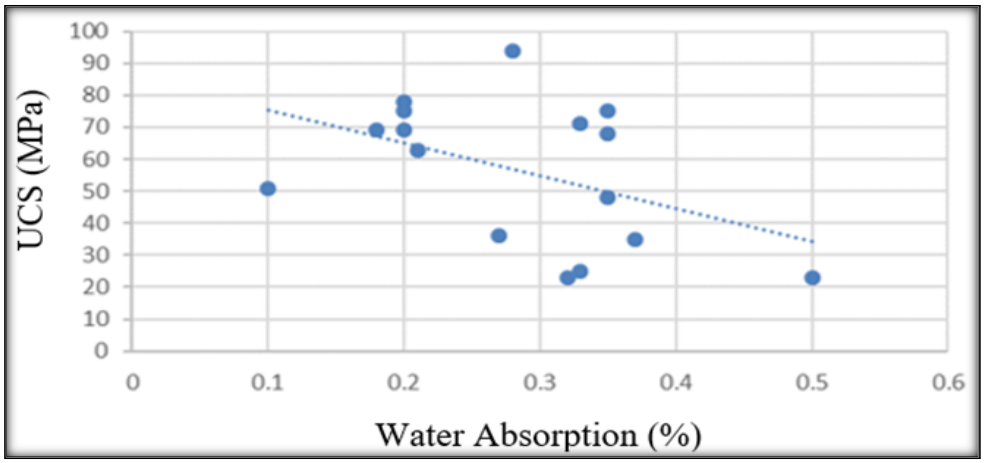

Figure 16. Relation between UCS and water absorption (%).

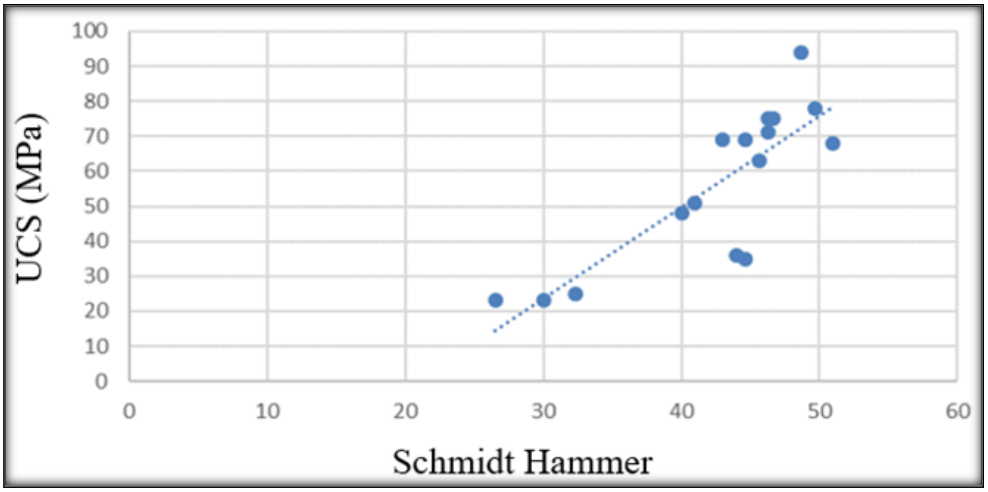

Figure 17. Relationship between UCS and Schmidt hammer.

Table 6. Comparison between UCS, water absorption and specific Gravity.

Sample number	Cube sample	UCS (MPa)	Water absorption (%)	Specific gravity
Pi1	Pi 1(a)	23	0.50	2.666
Pi2	Pi2(a)	35	0.37	2.674
	Pi2(b)	36	0.27	2.677
	Pi2(c)	71	0.33	2.680
Pi3	Pi3(a)	63	0.21	2.683
	Pi3(b)	75	0.20	2.688
	Pi3(c)	69	0.18	2.687
Pi4	Pi4(a)	51	0.10	2.694
	Pi4(b)	78	0.20	2.689
	Pi4(c)	94	0.28	2.676
Pi5	Pi5(a)	23	0.32	2.671
	Pi5(b)	25	0.33	2.671
	Pi5(c)	68	0.35	2.678

 doi:10.20944/preprints202409.1216.v

Pi6	Pi6(a)	75	0.35	2.634
	Pi6(b)	48	0.35	2.635
	Pi6(c)	69	0.20	2.784

4.3. Petrographic Analysis of the Inzari Formation

The systematic description and classification of rocks by microscopic analysis is known as petrography [22]. Under a polarized microscope, the petrographic laboratory investigated the petrographic characteristics of the rocks belonging to the Inzari Formation. Based on the gathered petrographic data, rocks are classified. In specimens, the rocks of the Insari formation range in hue from pale gray to dark gray. Alizarin red stain solution was used to color each thin segment [23]. Calcite gave off a pale pink to crimson color during the staining test, however dolomite did not show any staining.

The classification of limestone is determined based on the framework of depositional, biological, and diagenetic factor, shown in (Figure 18).

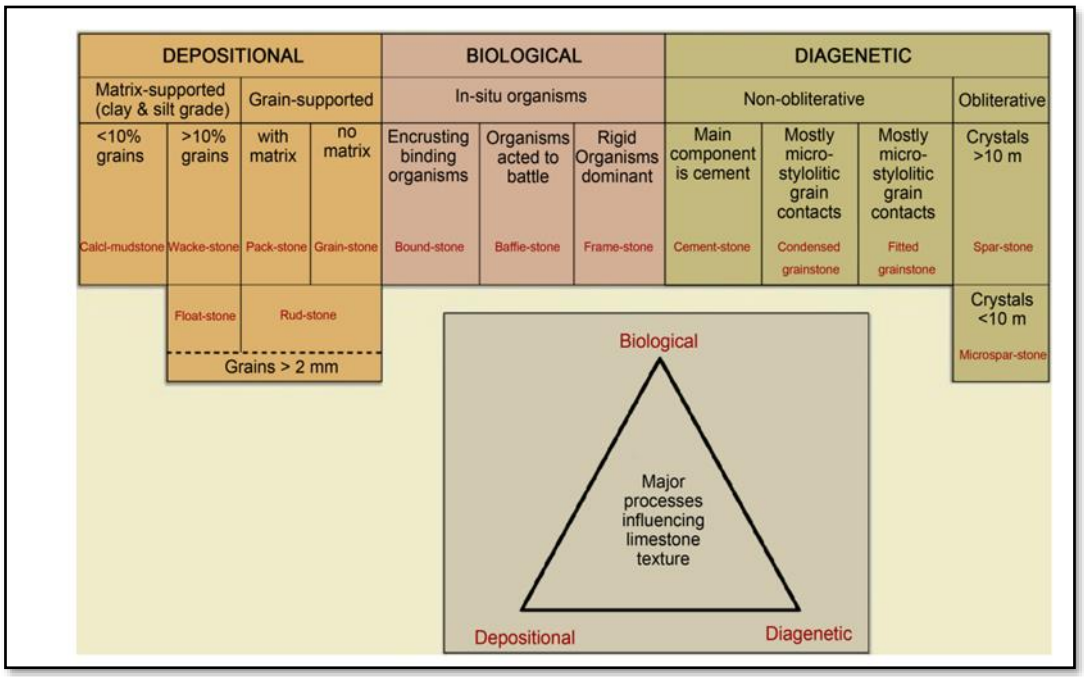

Figure 18. Classification framework of limestone.

According to the staining data, the majority of the studied rocks are made of calcite. In accordance with Dunham's classification, the dolomite samples were categorized [24]. For carbonate minerals, the Dunham's classification is based on the following three textural features.

(i) binding during deposition, a feature that sets bound stone apart from fine-grained carbonate rocks;

(ii) the characteristic that sets grain stone apart from muddy carbonates: the presence of sparry calcite cement in fine-grained carbonate minerals;

(iii) Grains are abundant in muddy carbonates, allowing for their division into mudstone, wacke stone, and pack stone. After the rock thin sections were analyzed for the petrographic description, these rock specimens were classified as "a siliciclastic mudstone" based on the texture, calcite cement (diabase), and mud matrix (micrite) [25]

The mineralogical composition of the studied samples is shown in Table 7.

Table 7. Mineralogical composition of the studied samples.

 doi:10.20944/preprints202409.1216.v

Sample name	Core sample	Micrite (%)	Sparite (%)	Calcite (%)	Quartz (%)	Opaque minerals (%)
Pi1	Pi1 (1)	60	15	14	9	2
	Pi1 (2)	56	19	13	9	3
Pi2	Pi2 (1)	62	13	16	6	3
	Pi2 (2)	59	20	10	10	1
Pi3	Pi3 (1)	61	14	13	10	2
	Pi3 (2)	55	20	13	9	3
Pi4	Pi4 (1)	60	21	12	5	2
	Pi4 (2)	59	19	9	10	3
Pi5	Pi5 (1)	61	15	14	8	2
	Pi5 (2)	59	18	15	7	1

4.3.1. Fractures

Almost every thin section had visible microfractures and bigger fractures. And smaller amounts of big fractures can also be visible in some thin sections in (Figure 19). The majority of these fractures run parallel to one another, but at certain points, they cross, forming a pattern of crisscross fractures [26]. They are nearly entirely composed of common minerals like silver and quartz. While some fractures contain quartz and spar, others mostly contain calcite cement. Some opaque minerals fill in some fissures.

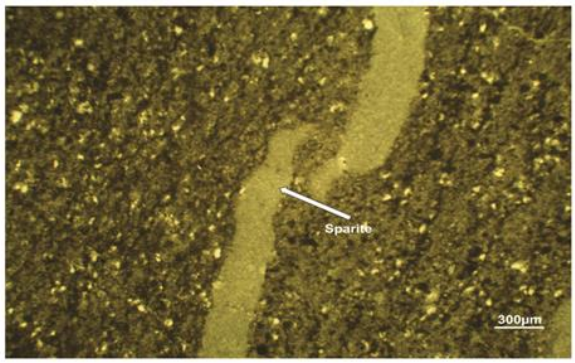

(a) Photomicrograph showing Sparite (PPL, 4x)

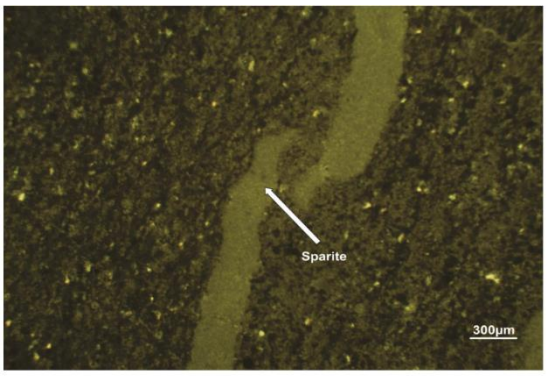

(b) Photomicrograph showing Sparite (PPL,4x)

 doi:10.20944/preprints202409.1216.v

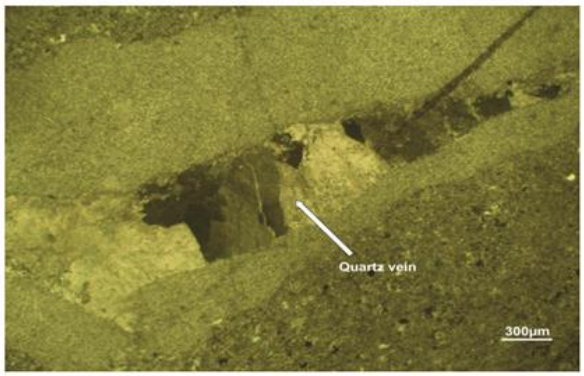

(c) Photomicrograph showing quartz vein (PPL, 4x)

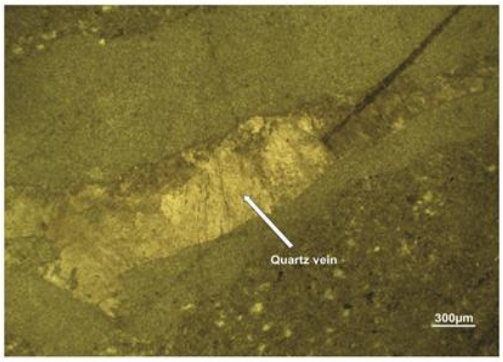

(d) Photomicrograph showing quatz (XPL,4x)

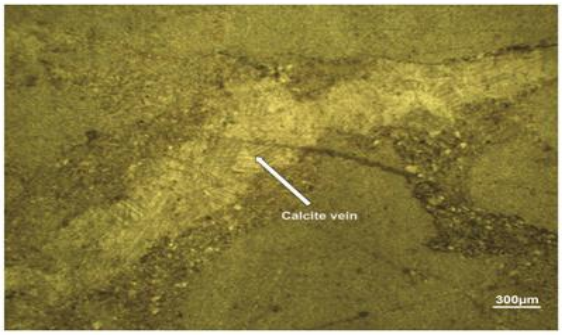

(e) photomicrograph showing calcite (PPL, 4x)

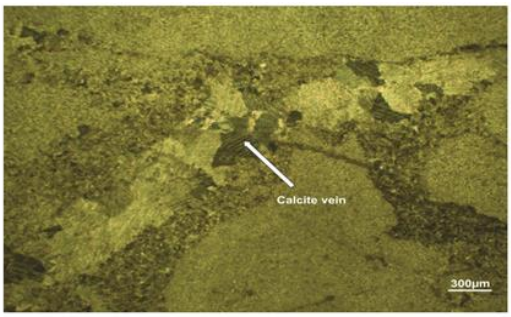

(f) Photomicrograph showing calcite (XPL, 4x)

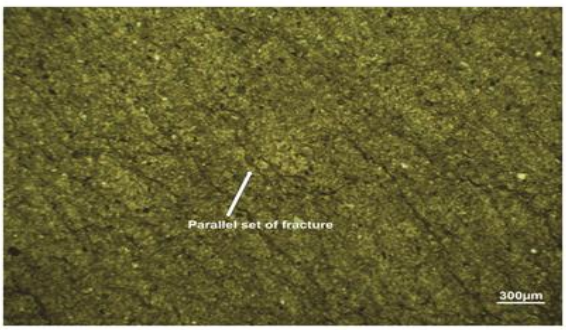

(g) Photomicrograph showing parallel set of fracture (PPL, 4x)

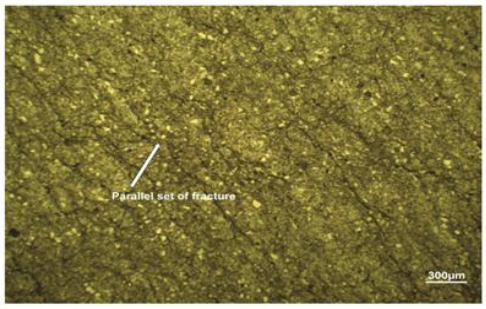

(h) Photomicrograph showing parallel set of fracture (XPL,)

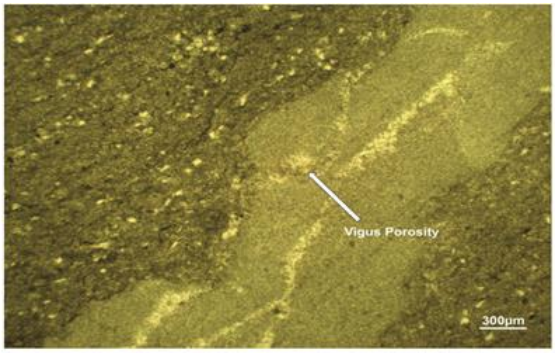

(i) Photomicrograph showing Vigus pores (PPL, 4x)

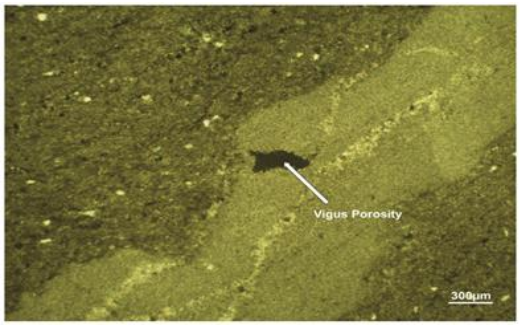

(j) Photomicrograph showing Vigus pores (XPL,4x)

Preprints.org (www.preprints.org) | NOT PEER-REVIEWED | Posted: 16 September 2024 doi:10.20944/preprints202409.1216.v

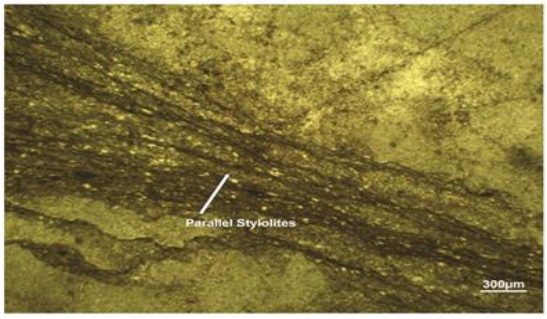

(k) Photomicrograph showing a parallel set of stylolites (PPL, 4x)

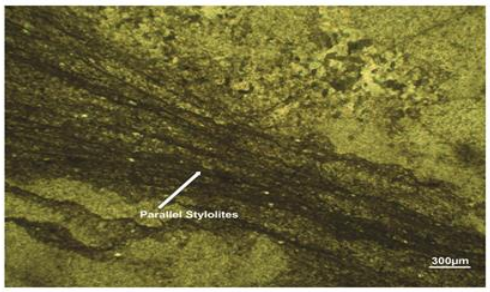

(l) Photomicrograph showing a parallel set of stylolites (XPL, 4x)

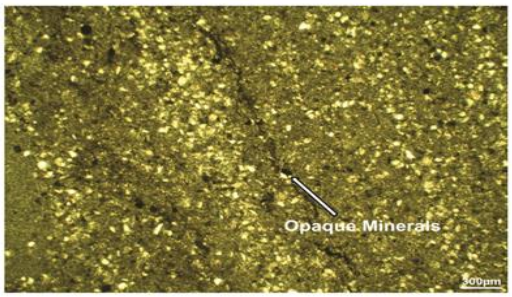

(m) Photomicrograph showing opaque mineral (PPL, 4x)

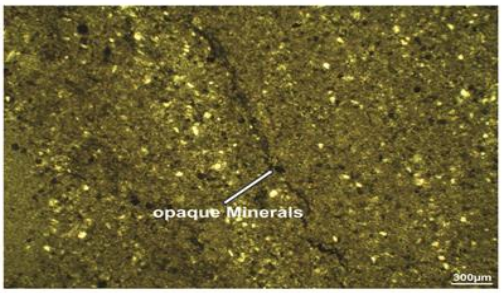

(n) Photomicrograph showing opaque mineral (XPL, 4x)

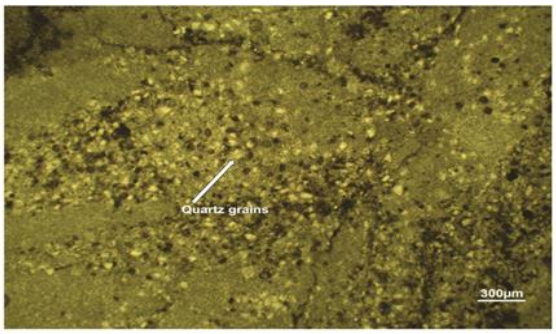

(o) Photomicrograph showing quartz cluster (PPL, 4x)

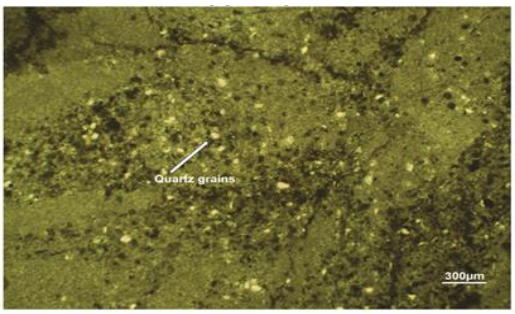

(p) Photomicrograph showing quartz cluster (XPL, 4x)

Figure 19. Photomicrograph showing of the studied samples.

4.3.2. Porosity

The porosity of the limestone samples in this study is significantly low, with a value of less than one (*porosity* <1), as detailed in Table 2. Pores in rock samples generally appears along fractures, where it is known as fracture porosity. Pore is colorless in plane-polarized light (PPL) and gives a dark black color in cross-polarized light (XPL) in (Figure 19i,j).

4.3.3. Micro-Stylolite

One kind of secondary (chemical) sedimentary structure is micro-stylolite, were also found in these rocks [27]. They are irregular suture-like connections that are created when pressure dissolves rocks in deep burial settings. They had concentrations of insoluble components and looked like narrow, jagged, and tooth-like seams. The direction of the maximal primary stress is perpendicular

 doi:10.20944/preprints202409.1216.v

to the stylolite. The stylolite in the studied thin sections is of an irregular form (plate) are parallel to one another, known as a parallel set of stylolites (see Figure 19k,I, and occasionally cross over one another, known as an irregular anatomizing set of stylolites.

4.3.4. Classification of the Studied Rocks

According to petrographic analyses, most of the rocks in the Inzari formation are fine-grained. Dunham's classification places the investigated rocks in the category of "Siliciclastic Mudstone." We use an alizarin-red stain solution to furtherly distinguish the studied rocks. Based on this identification result, these rocks are classified as mudstone because they contain a significant amount of mica minerals.

4.4. Discussions

Both the texture and the composition of these features depend on the petrographic feature. Generally, rocks with finer grain textures tend to be stronger than those with coarser textures. Since the majority of the tested rock samples have fine grains, they provide high strength values. While there are significant differences in the strength values of the samples under examination, all of the samples' UCS scores generally fall between moderately strong and very strong.

Rocks can be used for building if their values for UCS are higher than 35 MPa. Therefore, we can use the analyzed samples from the Inzari formation for construction purposes, as they have a UCS value greater than 35 MPa, and they have porosity and water absorption levels lower than 2%. The maximum amount of water that rock or aggregate can absorb before being used in construction is 2%, and more than 4% cannot be utilized in any situation, according to [28] fundamental rule. Given that the rock samples in this study have a lower water absorption value, it is deemed feasible to use it as construction aggregate [29].

According to the regulations of relevant departments in Pakistan, rocks can be used for heavy construction if their specific gravity is more than 2.55. Therefore, the studied rock sample with their high specific gravity value more than 2.55 is suitable for use as building material.

The occurrence of fractures and their orientations, the presence of micro-stylolite, the cementation along the fractures, and the modal mineralogical composition of the rocks are mostly responsible for these differences in the strength values. However, because the calcite and quartz mineral grains commonly fill these cracks, their strength values often are within an appropriate range for building.

In the case of thin and closed stylolite, a strength decrease is anticipated [30] The destabilizing effect of stylolite should be considered in geotechnical applications, especially in carbonate rocks where they are abundant. This is because water can permeate the rock and dissolve part of the stylolite's components, which makes them expand.

5. Conclusions

The present study focuses on the potential use of the Inzari formation as a supply of material for building endeavors. Many laboratory tests were conducted to assess its physical and mechanical characteristics, including specific gravity, water absorption, shear strength, porosity, uniaxial compressive strength, and uniaxial tensile strength. A thin-section examination was carried out to further clarify our comprehension of the mineral composition of samples. This study has drawn several main conclusions:

(1) The aggregate is suitable for use in construction projects, as shown by the estimated values for all physico - mechanical parameters, which meet international standards.
(2) Petrographic analyzes indicate that siliciclastic mudstone is a suitable classification for these rocks of the Inzari formation
(3) The rock of the Inzari formation can be used as concrete and asphalt aggregate.
(4) The rock of the Inzari formation appears to be between fairly strong and extremely strong based on the variation in UCS values.

(5) The rock of the Inzari formation with high specific gravity values, the low porosity, and water absorption, is a good material for construction.

(6) According to the petrographic features, the high micrite and calcite concentrations of the studied rock

(7) samples indicate that they can be used as both an asphalt aggregate and a concrete aggregate. These rocks have been used successfully as aggregates in asphalt and concrete, as well as in a variety of other building materials.

Acknowledgements: The research work in this paper was supported by the grants from the National Natural Science Foundation of China -Yalong River Joint Fund (No. U1765110), the Fundamental Research Funds for the Central Universities (22120180312).

Declaration of competing-interests: The authors declare that they have no known competing financial interests or personal relationships that could have appeared to influence the work reported in this paper.

References

1. Khan, N., Rehman, K., , *Petrophysical evaluation and fluid substitution modeling for reservoir depiction of Jurassic Datta Formation in the Chanda oil field, Khyber Pakhtunkhwa, northwest Pakistan.* Journal of Petroleum Exploration and Production Technology, 2019. 9(1**)**(159-176.).
2. Amuda, A., Uche, O., & Amuda, A., , *Physicomechanical Characterization of Basement Rocks for Construction Aggregate: A Case Study of Kajuru Area, Kaduna, Nigeria.* . IOSR Journal of Mechanical and Civil Engineering,, 2014. 11: p. 46-51.
3. Wang, J., Jung, W., Li, Y., & Ghassemi, A., , *eomechanical characterization of Newberry Tuf.* Geothermics, 2016. 63**,** : p. 74-96.
4. Ghobadi, M., & Babazadeh, R., 2015. Experimental Studies on the Effects of Cyclic Freezing–Thawing, Salt Crystallization, and Thermal Shock on the Physical and Mechanical Characteristics of Selected Sandstones. Rock Mechanics and Rock Engineering, 48, 1001-1016. , *Experimental Studies on the Effects of Cyclic Freezing–Thawing, Salt Crystallization, and Thermal Shock on the Physical and Mechanical Characteristics of Selected Sandstones.* Rock Mechanics and Rock Engineering, 2015. 48,: p. 1001-1016.
5. Khalid, P., Ehsan, M. I., Akram, S., Din, Z. U., & Ghazi, S., , *Integrated reservoir characterization and petrophysical analysis of cretaceous sands in lower Indus Basin, Pakistan.* . Journal of the Geological Society of India, 2018. **92,**: p. 465-470.
6. Aksoy, C., Ozacar, V., Demirel, N., Ozer, S., & Safak, S. , *Determination of instantaneous breaking rate by Geological Strength Index, Block Punch Index and power of impact hammer for various rock mass conditions.* . Tunnelling and Underground Space Technology,, 2011. **26,**(534-540).
7. Ademila, O., *Engineering geological evaluation of some rocks from Akure, Southwestern Nigeria as aggregates for concrete and pavement construction,Geology.* Geophysics and Environment,, 2019. 45,(31).
8. Přikryl, R., *Assessment of rock geomechanical quality by quantitative rock fabric coefficients: Limitations and possible source of misinterpretations.* Engineering Geology,, 2006. **87,**(149-162).
9. Aligholi, S., Lashkaripour, G., & Ghafoori, M., , *Estimating engineering properties of igneous rocks using semi-automatic petrographic analysis.* . Bulletin of Engineering Geology and the Environment, 2019: p. 78, 2299-2314.
10. Shah, S.A., & Qadir, A., , *Fracture Analysis of Rocks for Slope Stability Assessment in SiriKot Area, District Haripur, Khyber Pakhtunkhwa, Pakistan.* International Journal of Economic and Environmental Geology, , 2020. 11(3),: p. 53-56.
11. Tenze, D., Braitenberg, C., Sincich, E., & Mariani, P., , *Detecting the Elevated Crust to Mantle Section in the Kohistan-Ladakh Arc, Himalaya, from GOCE Observations,.* GOCE Observations,, 2014. 141,: p. 299-307.
12. Yeats, R.S., & Hussain, A. , *Timing of structural events in the Himalayan foothills of northwestern Pakistan.* . Geological society of America bulletin, , 1987: p. 99(2), 161-176.
13. Fahad, M., Iqbal, Y., Riaz, M., Ubic, R., & Redfern, S. A., , *Metamorphic temperature investigation of coexisting calcite and dolomit e marble—examples from Nikani Ghar marble and Nowshera Formation,.* Journal of Earth Science, 2016: p. 27, 989-997.
14. Iqbal, J., Ullah, I., Razzaq, A. M., Ghaffar, A., Murad, F., & Ahmed, J., , *Petrographic and sem-edx characterization of mafic-felsic plutonic rock of washapikaur west Raskoh Arc, Pakistan* Journal of Mountain Area Research, , 2022(7, 23-36).
15. Anjum, M.N., Shah, M. T., Ali, F., Hussain, E., & Ali, L., , *Geochemical studies of fluoride in drinking water of Union Council Ganderi, district Nowshera, Khyber Pakhtunkhwa, Pakistan.* World Applied Sciences Journal,, 2013(27(5),): p. 632-6.

 doi:10.20944/preprints202409.1216.v

16. Nisar, U.B., Ehsan, S. A., Farooq, M., Pant, R. R., Khan, N. G., Qaiser, F. U. R., & Butt, F. M.,, *Integrated Geoelectrical and Geological Investigation of a Quaternary Paleo-Depositional Environment in the Haripur Basin, Northern Pakistan.* Implications for Groundwater System. Geofluids,, 2023. **2023(1),** : p. 1057457.
17. Bubeck, A., Walker, R., Healy, D., Dobbs, M., & Holwell, D., , *Pore geometry as a control on rock strength.* Earth and Planetary Science Letters, , 2017(457,): p. 38-48.
18. Wang, J., Vandevyvere, B., Vanhessche, S., Schoon, J., Boon, N., & Belie, N.,, *Microbial carbonate precipitation for the improvement of quality of recycled aggregates.* Journal of Cleaner Production, 2017: p. 156, 355-366.
19. Malham, I., & Bureau, L., 2009. , *Density effects on collapse, compression, and adhesion of thermoresponsive polymer brushes. Langmuir:.* the ACS journal of surfaces and colloids, , 2009: p. 26 7, 4762-8.
20. Son, M., & Kim, M., , *Estimation of the Compressive Strength of Intact Rock Using Non-Destructive Testing Method Based on Total Sound-Signal Energy.* Geotechnical Testing Journal,, 2017(40, 643-657)
21. Fereidooni, D., & Khajevand, R.,, *Determining the Geotechnical Characteristics of Some Sedimentary Rocks from Iran with an Emphasis on the Correlations between Physical, Index, and Mechanical Properties.* Geotechnical Testing Journal,, 2018: p. 41, 555-573.
22. Li, Z., Zhang, X., Wei, Y., & Ali, M.,, *Experimental Study of Electric Potential Response Characteristics of Different Lithological Samples Subject to Uniaxial Loading. .* Rock Mechanics and Rock Engineering,, 2020: p. 54, 397-408.
23. Ademila, O., *Engineering geological evaluation of some rocks from Akure, Southwestern Nigeria as aggregates for concrete and pavement construction.* Geophysics and Environment, 2019: p. 45, 31.
24. Wright, V., *A revised classification of limestones. .* Sedimentary Geology, 1992. **76,**: p. 76, 177-185.
25. Shah, S.A., & Qadir, A., , *Fracture Analysis of Rocks for Slope Stability Assessment in SiriKot Area, District Haripur, Khyber Pakhtunkhwa, Pakistan.* 2020(11(3), 53-56.).
26. Gomez, L., & Laubach, S.,, *Rapid digital quantification of microfracture populations.* Journal of Structural Geology, 2006. **28,**: p. 408-420.
27. Stockdale, P., *Stylolites, primary or secondary? .* Journal of Sedimentary Research, 1943: p. 13, 3-12.
28. Afolagboye, L., Talabi, A., & Akinola, O., , *Evaluation of selected basement complex rocks from Ado-Ekiti, SW Nigeria, as source of road construction aggregates.* Bulletin of Engineering Geology and the Environment,, 2016. **75,** : p. 853-865.
29. Ademila, O., *Engineering geological evaluation of some rocks from Akure, Southwestern Nigeria as aggregates for concrete and pavement construction.* Geophysics and Environment, 2019. **45**: p. 31.
30. Baud, P., Rolland, A., Heap, M., Xu, T., Nicolé, M., Ferrand, T., Reuschlé, T., Toussaint, R., & Conil, N., , *Impact of stylolites on the mechanical strength of limestone.* 2016. **690,**: p. 4-20.